

HIGH PRESSURE LOW NOX EMISSIONS RESEARCH: RECENT PROGRESS AT NASA GLENN RESEARCH CENTER

Chi-Ming Lee

NASA Glenn Research Center, Cleveland, Ohio 44135 USA

Kathleen M. Tacina

NASA Glenn Research Center, Cleveland, Ohio 44135 USA

Changlie Wey

ASRC Aerospace Corporation, Cleveland, Ohio, 44135 USA

Abstract

In collaboration with U.S. aircraft engine companies, NASA Glenn Research Center has contributed to the advancement of low emissions combustion systems. For the High Speed Research Program (HSR), a 90% reduction in nitrogen oxides (NO_x) emissions (relative to the then-current state of the art) has been demonstrated in sector rig testing at General Electric Aircraft Engines (GEAE). For the Advanced Subsonic Technology Program (AST), a 50% reduction in NO_x emissions relative to the 1996 International Civil Aviation Organization (ICAO) standards has been demonstrated in sector rigs at both GEAE and Pratt & Whitney (P&W). During the Ultra Efficient Engine Technology Program (UEET), a 70% reduction in NO_x emissions, relative to the 1996 ICAO standards, was achieved in sector rig testing at Glenn in the world class Advanced Subsonic Combustion Rig (ASCR) and at contractor facilities. Low NO_x combustor development continues under the Fundamental Aeronautics Program.

To achieve these reductions, experimental and analytical research has been conducted to advance the understanding of emissions formation in combustion processes. Lean direct injection (LDI) concept development uses advanced laser-based non-intrusive diagnostics and analytical work to complement the emissions measurements and to provide guidance for concept improvement. This paper describes emissions results from flametube tests of a 9-injection-point LDI fuel/air mixer tested at inlet pressures up to 5500 kPa. Sample results from CFD and laser diagnostics are also discussed.

Nomenclature

FAR	[-]	fuel to air ratio
FN _{US}	[-]	fuel injector flow number
p	[kPa]	pressure
T	[K]	temperature

$\Delta p/p$	[-]	combustor pressure drop, $(p_3 - p_4)/p_3$
η_c	[-]	fuel combustion efficiency
ϕ	[-]	equivalence ratio

Subscripts

3	combustor inlet conditions
4	combustor exit conditions
ref	reference conditions

Introduction

Although most gas turbine engines currently used in commercial aircraft meet the 1996 International Civil Aviation Organization (ICAO) standard for emissions of nitrogen oxides (NO_x), NO_x emissions are still a concern due to their harmful effects on the atmosphere. NO_x contributes to the production of harmful ozone at ground level and in the troposphere, and also contribute to ground level smog. At the stratospheric altitudes that would be used for supersonic flight, NO_x contributes to the depletion of the protective ozone layer. To ensure combustion is as clean as possible and that aircraft gas turbines meet future more stringent regulations, low NO_x combustion concepts are being developed at NASA.

In addition to meeting more stringent emissions requirements, next-generation engine cycles will be required to simultaneously increase fuel efficiency. In order to achieve both efficiency and emissions goals NASA decided to support the development of high pressure cycle engines. Over the past two decades, NASA has sponsored both in-house research and collaborations with U.S. engine companies to develop advanced engines with higher efficiency that produce emissions. During the High Speed Research (HSR) program, the goal was to reduce NO_x emissions 90% relative to the then-current engine technology. Then, the Advanced Subsonic Technology (AST) project was initiated in the mid-1990's to increase fuel efficiency by 15% and reduce



Figure 1: 9-element fuel injector module

landing and takeoff cycle NO_x emissions to 50% of the 1996 ICAO standard while maintaining the present levels of carbon monoxide (CO) and hydrocarbon emissions. Following the AST Project, in the beginning of this century NASA introduced Ultra Efficient Engine Technology (UEET) Project to continue subsonic aircraft technology development with goals of 15% fuel efficiency improvement relative to current engines and 70% NO_x reduction.

NASA has investigated several combustion concepts to reduce NO_x emissions while maintaining high combustion efficiency: lean premixed prevaporized (LPP) combustion^{1,2}; rich burn-quick quench (RQL) combustion^{1,3,4}; catalytic combustion^{5,6}; lean direct injection (LDI) combustion; and rich front end combustion¹. LPP combustion met the HSR goal; the LPP, LDI, and RQL concepts all met the AST and UEET goals. This paper focuses on the LDI concept.

On the lean side of stoichiometric combustion, NO_x production is an exponential function of equilibrium flame temperature. Lean-burn low NO_x combustor concepts minimize the flame temperature by burning as lean as possible and avoiding local stoichiometric zones by mixing the fuel and air as well as possible. All of the combustor air, except for the liner cooling air, enters through the combustor dome. In lean, premixed, prevaporized (LPP) combustion, the fuel is mixed and vaporized upstream of the flame zone to ensure maximum mixing. However, due to the high pressures and temperatures and the wide-ranging duty cycles of aircraft gas turbine engines, autoignition and flashback into the premixing zone are a concern for LPP combustors. LDI combustion reduces the

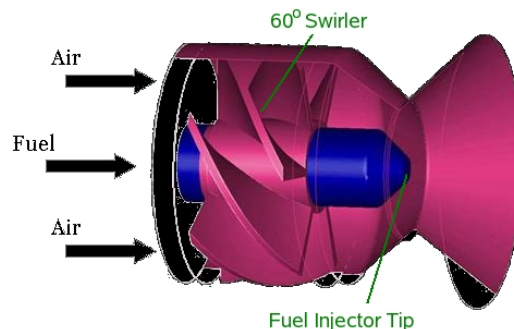


Figure 2: Fuel/air mixer element

potential for these problems by injecting the fuel directly into the flame zone. To ensure uniform mixing in LDI combustion, the fuel injector/swirler must be designed to produce small droplet sizes and quick mixing. Therefore, multi-injector LDI concepts --- where many small fuel/air mixers replace one conventional fuel injector --- have been studied. Under these conditions, NO_x emissions can approach those of LPP combustors¹. This paper focuses on very high pressure (up to 5500 kPa) tests of an in-house multipoint LDI fuel/air mixer concept developed under the AST program. The results are also compared to those from second-generation LDI sector and flametube tests.

Experimental Setup and Procedure

Fuel Injector/Mixer Configuration

The LDI module described here is a first-generation multipoint fuel-injection concept with 9 fuel/air mixers occupying a 76.2 mm x 76.2 mm square area, as shown in Figure 1. The 9 fuel/air mixers replace a single conventional fuel injector. Each fuel/air mixer is composed of a converging-diverging venturi section with an upstream swirler; a fuel injector is inserted at the center of each swirler (see Figures 1 and 2). The center-to-center distance between the fuel/air mixers is 25.4 mm. All of the air enters through the fuel/air mixers to provide an overall lean burning zone. Each fuel/air mixer provides rapid mixing of fuel and air and results in a small recirculation zone to stabilize the combustion process; the uniform mixing and short recirculation zone result in ultra low NO_x emissions.

Swirlers with helical, axial blades are used for mixing and generating a recirculation zone. All swirlers are co-rotating with a blade angle of 60°, as shown in Figure 2. The blades have an inside diameter of 9.4 mm and an outside diameter of 22 mm. The calculated swirl number, as defined by Beer and Chigier⁷, is 1.02. The measured effective area of the air swirler array is 940 mm².

Each fuel injector is of the simplex type. A similar fuel injector design was used in both the

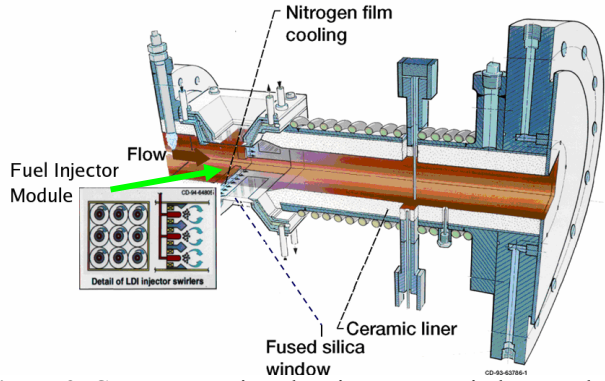


Figure 3: CE-5 test section showing quartz windows and a detail of the fuel injector module

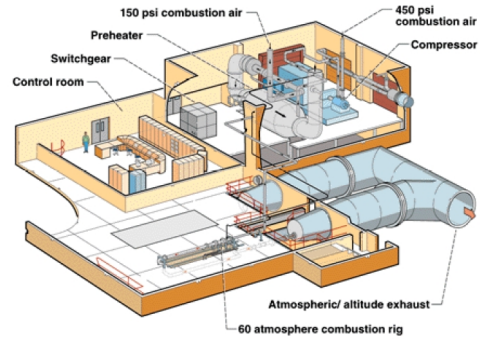
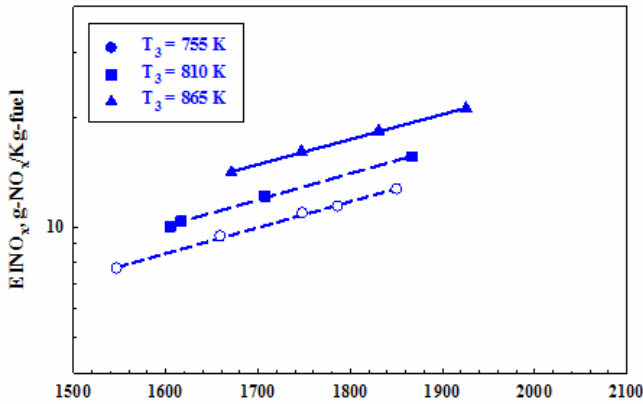
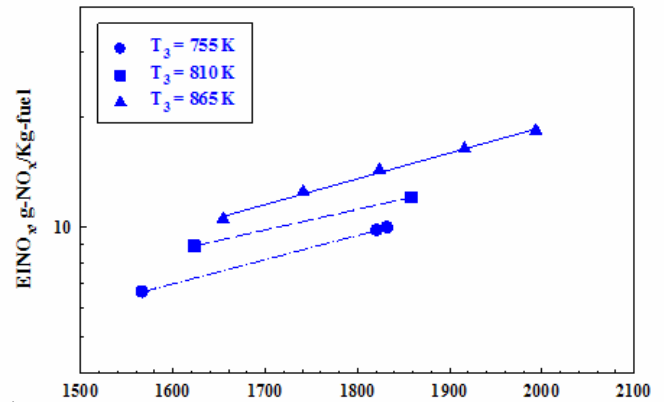


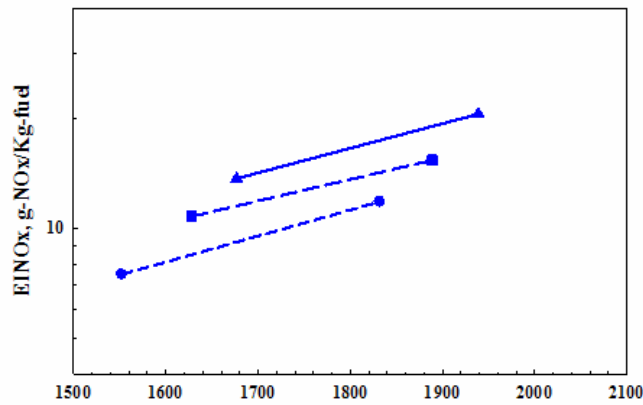
Figure 4: Advanced Subsonic Combustion Rig (ASCR)



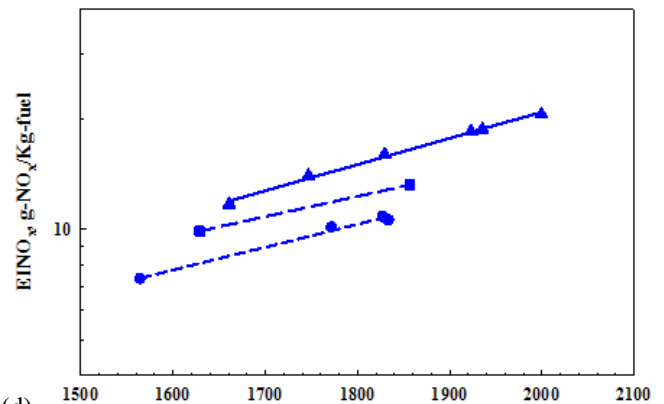
(a)



(c)



(b)



(d)

Figure 5: NO_x, EI as a function of adiabatic flame temperature at a pressure drop, $\Delta p/p_3$, of 7%, and an inlet pressure of (a) 5500 kPa, (b) 5200 kPa, (c) 3800 kPa, and (d) 4500 kPa.

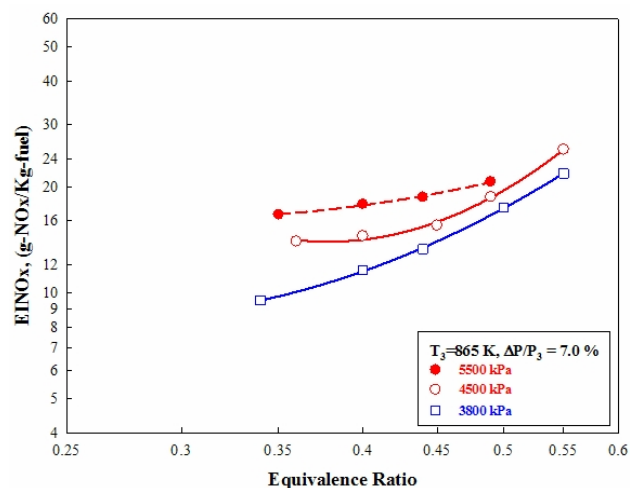


Figure 6: NO_x emissions as a function of equivalence ratio and inlet pressure.

ASCR and CE-5 tests. For the ASCR tests, the flow number FN_{US} (as defined by Lefebvre⁸) of the each fuel injector is 9, and the fuel orifice diameter is 1.97 mm. For the CE-5 tests, FN_{US} is 2.9

Experimental Installation

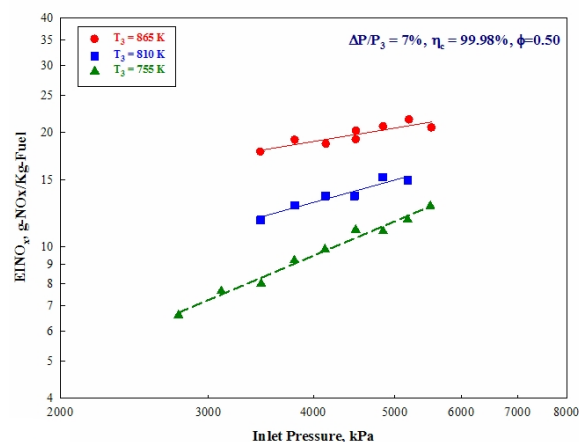
Testing was done in two facilities at NASA Glenn Research Center: CE-5 and the Advanced Subsonic Combustor Rig (ASCR).

CE-5 is a high pressure/high temperature combustion facility capable of supplying air at up to 2100 kPa, 4.5 kg/s, and 870 K. For the tests described in this paper, CE-5 was configured with a 76.2-mm by 76.2-mm square flامتube. As shown in Figure 3, the combustion section can be configured with 4 quartz windows, spaced 90° apart, for non-intrusive laser diagnostics; each window is 38.1-mm by 50.8-mm. If laser diagnostics are not desired, blanks can replace the quartz windows. The hot combustion products are quenched with water and then vented to the altitude exhaust system, which was run at atmospheric pressure.

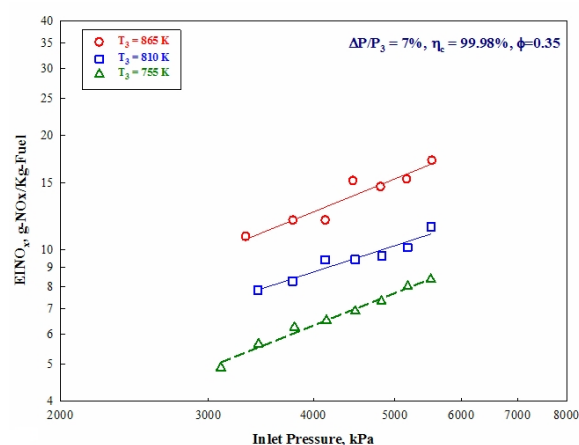
ASCR is a very high pressure/high temperature combustion facility capable of supplying air at up to 5500 kPa, 17 kg/s, and 975 K (see Figure 4). Before being exhausted to the atmosphere, the hot combustion products are quenched with water. See Bianco⁹ for further details.

Results and Discussion

This section is divided into three parts. First, NO_x emissions measurements taken in the high pressure/high temperature ASCR facility are presented. Then, a correlation for NO_x emissions as a function of combustor conditions is given and



(a)



(b)

Figure 7: NO_x emissions as a function of inlet pressure and inlet temperature at equivalence ratios of (a) 0.5 and (b) 0.35.

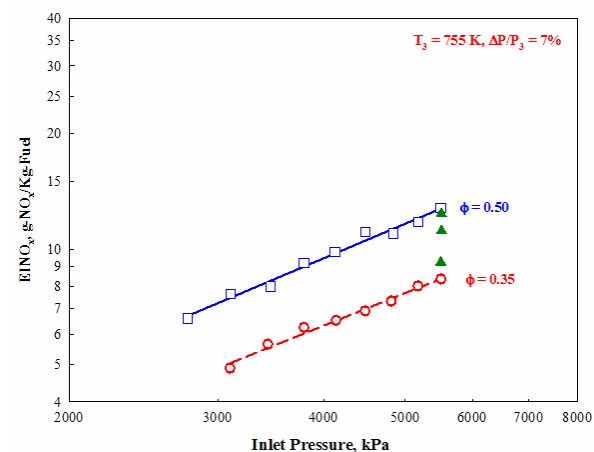


Figure 8: NO_x emissions as a function of inlet pressure at an inlet temperature of 755 K and a pressure drop of 7%.

compared to both medium pressure/high temperature data taken in CE-5 and the high pressure/high temperature ASCR data. Finally, insights from CFD calculations and optical diagnostic measurements are used to explain why second generation LDI designs have lower emissions than the first generation LDI design described in this report.

Emissions Data

Figures 5-8 plot the NO_x emissions as a function of combustor conditions. NO_x values are given as emissions index, defined as grams of NO_x per kilogram of fuel.

In Figure 5, the log of the NO_x emissions index is plotted as a function of adiabatic flame temperature T_4 for inlet temperatures T_3 of 755 K (circles), 810 K (squares), and 865 K (triangles) and inlet pressures p_3 of 5500 kPa, 5200 kPa, 3800 kPa, and 4500 kPa. Note that the log of NO_x appears to vary linearly with adiabatic flame temperature, which indicates that, as expected, NO_x emissions are an exponential function of adiabatic flame temperature.

Figure 6 plots the log of NO_x emissions index as a function of the log of equivalence ratio at an inlet temperature of 865 K and inlet pressures of 3800 kPa (squares), 4500 kPa (open circles), and 5500 kPa (closed circles). At the 5500 kPa, NO_x emissions seem to be a much weaker function of equivalence ratio than they are at lower pressures.

The log of the NO_x emissions index is plotted against the log of the inlet pressure in Figures 7 and 8. In part (a) of Figure 7, the equivalence ratio is 0.50 and the inlet temperatures are 755 K (triangles), 810 K (squares), and 865 K (circles); in part (b), the same three inlet temperature curves are plotted but the equivalence ratio is 0.35. In Figure 8, the inlet temperature is kept constant at 755 K, but equivalence ratios of 0.35 (circles) and 0.50 (squares) are plotted together. The log of the NO_x emissions index seems to be a linear function of the log of the inlet pressure, indicating that NO_x emissions are a power function of inlet pressure.

NO_x correlation for data comparison

The NO_x data are compared to two correlations that give the NO_x emissions index as a function of inlet temperature, inlet pressure, pressure drop, and fuel-to-air ratio. The first correlation was developed for this LDI configuration using the high temperature, high pressure data taken in ASCR, and is given by:

$$EINO_x = 0.104 \exp(T_3/185) FAR^{1.32} p_3^{0.68} (\Delta p/p_3)^{-0.36}, \quad (1)$$

The second correlation,

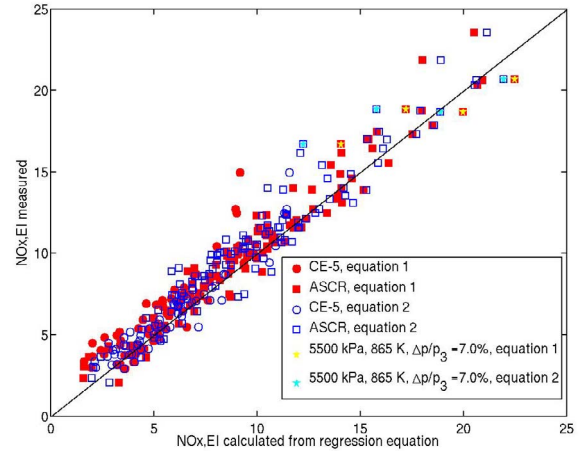


Figure 9: Comparison of measured and calculated NO_x emissions index.

$$EINO_x = 1.359 \exp(T_3/194) FAR^{1.69} p_3^{0.595} (\Delta p/p_3)^{-0.565}, \quad (2)$$

is almost identical to the NO_x severity parameter developed by Wey¹⁰ using several multipoint LDI configurations: the only difference is the coefficient, 1.359, which was found using the high pressure, high temperature ASCR data. All of the other constants in equation 2 were found using several different data sets taken during the AST.

Figure 9 plots the measured NO_x emissions index against the NO_x emissions index calculated from equations 1 (filled red symbols) and 2 (open blue symbols). The high pressure, high temperature ASCR data is plotted using squares, and the medium pressure, high temperature CE-5 data is plotted using circles. Both correlations fit the high pressure, high temperature ASCR data quite well ($R^2=0.95$ for equation 1 and 0.92 for equation 2). However, equation 2 fits the medium pressure, high temperature data taken in CE-5 ($R^2=0.90$) much better than equation 1 ($R^2=0.78$). Since equation 1 fits only the high pressure data well, but equation 2 fits both the high pressure and the medium pressure data well, the correlation equation 2 is a more general equation.

Finally the four points on the 5500 kPa curve in Figure 6 are plotted a second time in Figure 9 using yellow stars for the correlation in equation 1 and cyan stars for the correlation in equation 2. Although Figure 6 seems to indicate that NO_x emissions are a weaker function of equivalence ratio at high pressure and temperature, Figure 9 shows that NO_x correlation equations 1 and 2 still predict NO_x emissions fairly well.

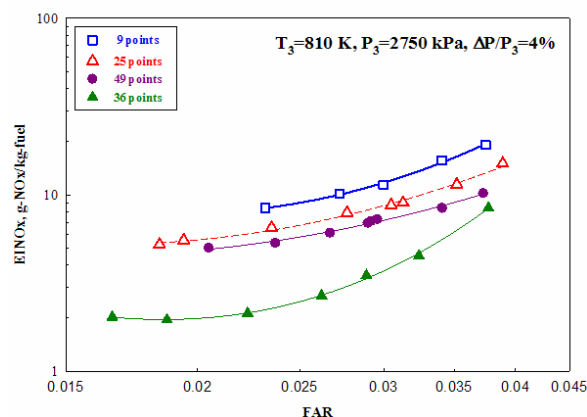


Figure 10: Comparison of first generation 9-point and second generation LDI flametube NOx emissions.

Analysis and Comparison with Second Generation LDI

The data presented here were the first measurements taken in the high pressure/high temperature ASCR facility and showed that this facility operated well under these high pressure conditions. In addition, these were also the first emissions measurements on the LDI concept at very high pressure conditions and showed that LDI combustion produced low NOx emissions varied smoothly with inlet pressure, even at pressures up to 5500 kPa. The measurements also showed that the operability and durability of LDI was good even at high pressure/high temperature conditions.

Based on the success of this first generation LDI injector, second generation LDI geometries have been designed and tested^{14,15}. Included in the second generation are designs that incorporate more injection points in the same cross section area to minimize the recirculation zone and the residence time effect. The smaller recirculation zone and decrease in residence time results in a decrease in NOx emissions.

Figure 10 compares first and second generation LDI emissions; the data shown are corrected to a constant inlet temperature of 810 K, inlet pressure of 2750 kPa, and $\Delta p/p_3$ of 4%. The first generation 9-

	Power	Time	Total pressure at station 3	$\Delta p/p_3$
	%	min	kPa	%
SLTO	100.0	0.7	969.8	4
Climb	85.0	2.2	933.7	4
Approach	30.0	4	740.4	4
Idle	7.0	26	615.4	4

Table 1: UEET large engine LTO cycle

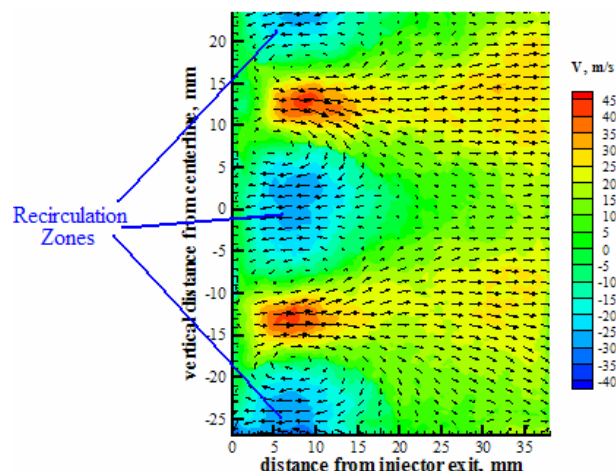


Figure 11: Velocity field compiled from 200 PIV images.

point LDI (hollow blue squares) has higher NOx emissions than any of the three second generation LDI concepts shown, which are: the 25-point LDI (hollow red triangles), the 49-point LDI (solid purple circles), and 36 points LDI (solid green triangles). In addition, all of the second generation multi-injection LDI concepts have a better operability range (i.e., wider FAR range) than the first generation LDI concepts. The 36-point has the best NOx emissions reduction potential. The 49-point LDI had disappointing NOx emission results; after testing we examined the injector with the designer and found that there were a few blockages inside the fuel passage which caused non-uniform fuel/air mixing. In addition, all of the second generation multi-injection LDI designs have better operability range than the first generation (i.e., a wider FAR range).

Table 1 shows a hypothetical engine cycle for the NASA Ultra Efficient Engine, the ICAO landing-take off (LTO) characteristic for that engine is calculated for both first and second generation LDI concepts. Assuming 15% cooling air for the engine, the LTO NOx is 63% below the 1996 ICAO standard for the first generation LDI, and 71% below 1996 ICAO standard for the second generation LDI.

We applied advanced laser diagnostics techniques⁶ and the in-house National Combustion Code⁷ to better understand fuel injector design.

Particle imaging velocimetry (PIV) was used to measure the velocity field downstream of the injector. This allowed the size and location of the recirculation zones to be identified. Figure 11 shows side view contours of axial velocity at locations ranging from 3 mm to 35 mm downstream of the injector exit plane; this image was taken in unfueled cold flow at an inlet temperature of 617 K, inlet pressure of 1030 kPa, and pressure drop of 4%.

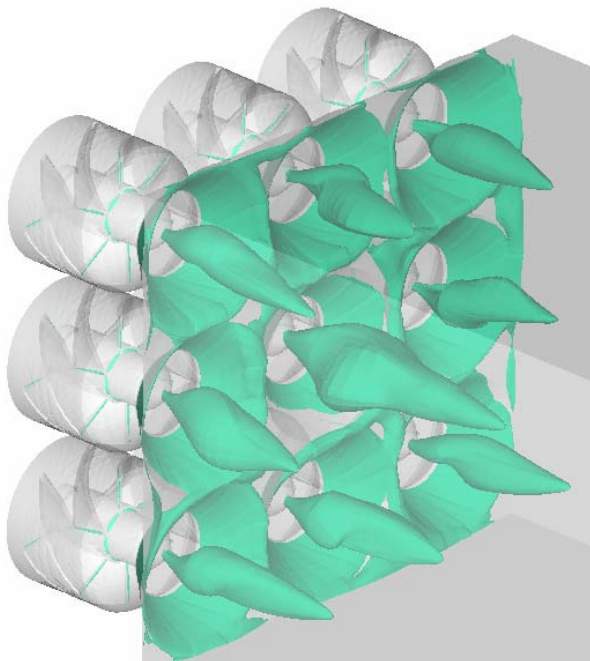


Figure 12: Nine-point, LDI results that show zero axial velocity iso-surfaces.

From these images we observe that the heart of the flow recirculation zone occurs between 5-7 mm from the injector exit and provides confirmation of the presence of recirculation zone immediately downstream of each injection point. Note the three strong recirculation zones (indicated by the arrows to the left and by light blue and blue colors) approximately 7 mm from the injector exit. More details are given in Hicks et al¹¹.

This strong recirculation zone was also calculated using the National Combustion Code. The recirculation zones associated with the injection points are illustrated by the iso-surfaces of zero axial velocity in Figure 12 computed by Davoudzadeh et al¹².

Summary

This paper presents results from the first combustion test done in the high pressure/high temperature ASCR facility at NASA Glenn Research Center. This test was also the first high pressure/high pressure test of the LDI concept and showed that LDI had good operability and durability even at pressures up to 5500 kPa. NO_x emissions varied smoothly with inlet pressure, flame temperature, and equivalence. The limited number of data points at very high pressure and temperature conditions indicated that, at very high pressures, NO_x emissions are a weaker function of equivalence ratio than they are at lower pressures. A correlation for NO_x emissions as a function of inlet temperature, inlet pressure, pressure drop, and fuel/air ratio was

developed and showed high correlation with the measured NO_x emissions at high pressure and temperature. However, another correlation that was based on the Advanced Subsonic Technology Program (AST) NO_x severity parameter had almost as high a correlation with the high pressure/high temperature data and a much higher correlation with the medium pressure/high temperature data.

This paper also summarizes LDI concept development through design, analysis, and testing. In the LDI concept, fuel is injected directly into the primary zone; this minimizes auto-ignition potential. However, in order to achieve low NO_x, it is important to have fine atomization from fuel and uniform mixing from fuel and air. In addition, a small recirculation zone and a short flame zone are also critical for NO_x reduction. Based on NO_x reduction achieved by the first generation of LDI concepts, a second generation of LDI concepts was developed to further reduce NO_x emissions.

References

1. Tacina, R.R., (1989). "Low NO_x Potential of Gas Turbine Engines," AIAA 89-0550, 38th Aerospace Sciences Meeting, Reno, NV, 1990.
2. Lee, C.-M., Bianco, J., Deur, J.M., and Ghorashi, B., (1992). "Nitric Oxide Formation in a Lean Premixed Prevaporized Jet A/Air Flame Tube: an Experimental and Analytical Study", NASA/TM---105722.
3. Chang, C.T, and Holdeman, J.D., (2001). "Low Emissions RQL Flametube Combustor Test Results," NASA/TM---2001-211107.
4. Peterson, C.O., Sowa, W.A., and Samuelson, G.S. (2002). "Performance of a Model Rich Burn-Quick Mix-Lean Burn Combustor at Elevated Temperature and Pressure," NASA/CR--2002-21192.
5. Brabbs, T.A., and Gracia-Salcedo, C.M., (1989). "Fuel-Rich Catalytic Combustion of Jet-A Fuel -- Equivalence Ratios 5.0 to 8.0," NASA TM/101975.
6. Rollbuhler, R.J., (1991). "Fuel-Rich, Catalytic Reaction Experimental Results," NASA/TM 104423.
7. Beer, J.M., and Chigier, N.A., (1972). *Combustion Aerodynamics*, John Wiley and Sons, Inc., New York.
8. Lefebvre, A.H., (1998). *Gas Turbine Combustion*, Taylor and Francis, Philadelphia.
9. Bianco, J., (1995). "NASA Lewis Research Center's Combustor Test Facilities and Capabilities," AIAA 1995-2681, 31st AIAA/ASME/SAE/ASEE Joint Propulsion Conference, San Diego, CA.
10. Wey, Changlie (2004), "A High Pressure and

- High Temperature NO_x Correlation", paper in progress.
11. Hicks, Y. R., Anderson, R.C., Locke, R.J., and Wey, C., (2006). "Experimental Study to Characterize a Baseline Nine-Point Lean Direct Injector," Spring Technical Meeting of the Central States Section of the Combustion Institute, Cleveland, OH, 2006.
 12. Davoudzadeh, F., Liu, N.-S., and Moder, J.P., (2006). "Investigation of Swirling Air Flows Generated by Axial Swirlers in a Flame Tube," GT-2006-91300, ASME Turbo Expo 2006: Power for Land, Sea, and Air, Barcelona, Spain, 2006.
 13. Iannetti, A. and Moder, J., "Analysis of MEMS-LDI Technology Using the National Combustion Code," AIAA 2005-169, 43rd AIAA Aerospace Sciences Meeting and Exhibit, Reno, NV, 2005.
 14. Tacina, R., Wey, C., Laing, P., and Mansour, A., (2002). "A Low NO_x Lean-Direct Injection, MultiPoint Integrated Module Combustor Concept for Advanced Aircraft Gas Turbines," NASA/TM—211347.
 15. Tacina, R., Mao, C.-P., and Wey, C., (2003). "Experimental Investigation of a Multiplex Fuel Injector Integrator for Low Emission Combustors," AIAA 2003-0287, 41st Aerospace Sciences Meeting and Exhibit, Reno, NV, 2003.